

Onset of slow dynamics in difluorotetrachloroethane glassy crystal

F. Affouard, E. Cochin, F. Danède, R. Decressain, M. Descamps

Laboratoire de Dynamique et Structure des Matériaux Moléculaires,

CNRS UMR 8024, Université Lille I,

59655 Villeneuve d'Ascq Cedex France

W. Haeussler

Institut Laue-Langevin, 38042 Grenoble, France

Abstract

Complementary Neutron Spin Echo and X-ray experiments and Molecular Dynamics simulations have been performed on difluorotetrachloroethane (CFC12-CFC12) glassy crystal. Static, single-molecule re-orientational dynamics and collective dynamics properties are investigated. The orientational disorder is characterized at different temperatures and a change in nature of rotational dynamics is observed. We show that dynamics can be described by some scaling predictions of the Mode Coupling Theory (MCT) and a critical temperature T_c is determined. Our results also confirm the strong analogy between molecular liquids and plastic crystals for which α -relaxation times and non-ergodicity parameters are controlled by the non trivial static correlations as predicted by MCT.

I. INTRODUCTION

Understanding of the mechanisms leading to the glass transition has been a subject of intense research in recent years and it is still a matter of numerous theoretical and experimental studies [1]. A fundamental question particularly concerns the microscopic description of the precursor cooperative mechanisms which develop in the high temperatures pico-nanosecond regime (ps-ns) far above the glass transition temperature T_g . It is now commonly suspected, mainly from theoretical and numerical results, that dynamical behaviours of glass-forming systems could be described by involving two characteristic temperatures [2]: i) T_A (T_S or T_x are also seen) corresponding to the onset of slow dynamics where non-exponential relaxation and non-Arrhenius behavior emerge [2]. First appearance of rotational heterogeneity are also reported [3]. The role of T_A in the vitrification process is still not completely understood but it is often considered as the temperature below which dynamics are influenced by the potential energy landscape [2]. ii) T_c , the critical temperature predicted by the Mode Coupling Theory MCT [4]. In the last two decades, enormous work has been devoted to this theory and it is so far the only one which provides a microscopic description of simple liquids. The intrinsic basis of MCT states that the behaviour of any time-dependent correlators describing the dynamics of the system is only controlled by its static density correlator *i.e* $S(Q)$ and predicts the existence of a critical temperature T_c indicating a bifurcation from ergodic to non-ergodic dynamics. The role of $S(Q)$ and the scaling properties predicted by MCT approaching T_c have been successfully validated in numerous experiments and molecular dynamics (MD) simulations [5]. However, no sharp transition is observed at T_c itself owing some activated processes not included in the theory which restores ergodicity. Thus, T_c is also associated to a dynamical crossover to a 'landscape-dominated' regime in which diffusion processes can be described in terms of thermally activated jumps.

Most of the glassformers are molecular liquids and accordingly possess both translational and rotational degrees of freedom (TDOF and ODOF). Approaching the glass transition, the coupling between TDOF and ODOF is far from being understood and the precise role of the ODOF remains unclear as demonstrated by the so-called low-temperature translation-rotation paradox [6, 7]. MCT has been initially developed to provide a microscopic understanding of simple atomic liquids. However, general predictions have also been successfully validated for molecular compounds. Recently, some extensions of MCT called molecular mode coupling theory (MMCT) [5] have been proposed to take ODOF into account: one diatomic probe molecule in an atomic liquid [8], liquids made of linear molecules [9] or water [10] to cite only a few. The authors have particularly shown that some of the basic predictions of MCT still hold owing to TDOF/ODOF coupling. As revealed by recent MD investigations [11, 12] performed on orthoterphenyl (OTP), coupling of the rotational dynamics to the center-of-mass motion can be complex.

An alternative to the glassforming molecular liquids is offered by at least two partially disordered systems which provide an interesting solution in order to investigate only ODOF during the freezing process :

i) The so-called *orientational glasses* such as $\text{Ar}_{1-x}(\text{N}_2)_x$ or $(\text{KCN})_x(\text{KBr})_{1-x}$ mixed crystal where rotational motions are frustrated by a quenched disorder externally imposed by a dilution [13]. K. H. Michel and coworkers [14] developed a MCT for these systems which involved the interplay of rotational-translational and rotational-strains coupling where strains result from the substitutional disorder.

ii) *Glassy crystals* [15] such as cyanoadamantane [16], ethanol [17, 18], orthocarborane [19] or cyclooctanol [20] which are true rotational analogs of canonical liquid glassformers. These systems are generally composed of globular molecules and exhibit a partially disordered phase, called plastic, which possesses a crystalline translational order and a dynamical orientational dis-

order. They can be rapidly cooled from the plastic phase and exhibit a step of the specific heat at the calorimetric temperature T_g or a non-Arrhenius behavior of the rotational relaxation times.

No microscopic theory has been developed for plastic crystals so far. However, in [21, 22, 23], we have particularly shown from NMR and Raman experiments, and MD computer simulations that some predictions of the idealized version of the MCT (critical temperature T_c and time scaling laws) were able to describe relatively well rotational dynamics of different plastic crystals. It should be noted that the other remarkable temperature T_A was also identified. These intriguing previous results call for new investigations to clarify the similarity between slow dynamics behaviour of plastic crystals and molecular liquids and in particular to discuss the role of the static correlations $S(Q)$. In this paper, we present for the first time results of Neutron spin-echo (NSE) and X-ray experiments and MD simulations of the glassy crystal difluorotetrachloroethane (DFTCE). This compound is composed of simple molecules $\text{CFCl}_2 - \text{CFCl}_2$ close to dumbbells extensively used in MD calculations as prototype of molecular glass-formers liquids [24, 25, 26]. DFTCE has been experimentally widely studied and presents a rich variety of unusual properties. DFTCE exhibits a glass transition of the overall rotation of the molecules at $T_g = 86$ K [27]. Two additional heat anomalies are found at 60 and 130 K and associated respectively to a sub- T_g β process and the freezing of the transformation between *trans* and *gauche* conformation of the molecule. Changes concerning the nature of dynamics in this system has been reported from NMR experiments [29], Brillouin and dielectric spectroscopy [28]. In this latter investigation, a crossover from individual to correlated rotational motions was particularly suggested.

II. EXPERIMENTS AND DETAILS OF THE SIMULATION

The samples used in both X-ray and NSE experiments consist of commercial 1,2-difluorotetrachloroethane purchased from Sigma-Aldrich and purified by melting zone.

The X-ray diffraction experiment was performed on a laboratory diffractometer equipped with an INEL curved sensitive detector CPS 120 made up of 4096 channels and allowing us to record simultaneously X-ray diffraction on a 2θ range of about 120 deg. The incident beam was monochromatized with a bent of quartz crystal which selects the K_{α_1} wavelength of a Cu X-ray tube ($\lambda = 1.54056 \text{ \AA}$). Powder DFTCE was introduced in Lindemann glass capillary of 0.5 mm in diameter. It was mounted on the axis of the diffractometer and rotated during the experiment in order to reduce the effect of preferential orientation. The correspondence between the channel number and the 2θ angle was determined by a preliminary X-ray experiment of cubic $\text{Na}_2\text{Ca}_2\text{Al}_2\text{F}_{14}$ (NAC) [30] with a cubic spline interpolation between the Bragg peaks of NAC. Low temperatures were achieved by placing the sample into a gaseous nitrogen flow at the required temperature. Using this procedure, the sample is quenched within a few seconds, and its temperature can be controlled within 0.5 K between 110 K and 300 K. In the present experiment, the X-ray pattern was recorded at 140 K during 3600 s for a sample quenched at 2K/min.

The NSE experiments were performed on the IN11 spectrometer at the Institut Laue-Langevin (ILL), Grenoble, France. We used the multidetector version of IN11 which allows simultaneous measurements at different scattering angles. A setup with an incident wavelength of $\lambda = 5.5 \text{ \AA}$ ($\Delta\lambda/\lambda \simeq 16 \%$) gave access to wave numbers approximately between 1.28 and 1.72 \AA^{-1} and we covered the time range 8 ps - 1 ns. We made measurements of the coherent signal of polycrystalline systems filled into a flat Al container from $T = 130$ to 220 K in steps of 10 K. For normalization, a resolution scan of the elastic scattering was realized at $T = 5 \text{ K}$ in the glassy phase and all data were divided by the polarization at this temperature. Two samples of different mass identified as A ($m \simeq 0.33 \text{ g}$) and B ($m \simeq 2 \text{ g}$) were investigated. Although preliminary measurements showed that transmission of sample A was better, 93% to be compared to 77% obtained for sample B, this latter was preferred for most of the measurements since its scattering

signal was more intense. Unfortunately, only data obtained from sample A are available at $T = 130$ and 140 K.

MD calculations were performed on a system of $N = 686$ ($7 \times 7 \times 7$ bcc crystalline cells) molecules. Each DFTCE molecule $\text{CFCl}_2 - \text{CFCl}_2$ is described by its 8 atoms and considered as a rigid unit. They interact through a Buckingham short range atom-atom potential (see parameters in table I) and the electrostatic contributions have been neglected since the DFTCE molecule possesses a weak dipolar moment. No structural or dynamical change has been found for a system where electrostatic interactions are taken into account. It should be noted that both structure and dynamics were found in good agreement with experimental results (see figures 1 and 3). Newton's equations of motion were solved with a time step of $\Delta t = 5$ fs. We worked in the NPT statistical ensemble with periodic boundaries conditions where the simulation box is allowed to change in size and shape. MD simulations were done for a sample corresponding to the DFTCE orientationally disordered phase at 14 different temperatures from $T = 130$ to 260 K in steps of 10 K. It should be mentioned that our very simple DFTCE model allows us to perform very long MD runs of about 50 ns.

In this paper, single-molecule reorientational dynamics of DFTCE will be obtained from the first two self angular correlation functions $C_{l=1,2}$ [24] defined as:

$$C_l(t) = \frac{1}{N} \sum_{i=1, N} \langle P_l(\vec{u}_i(t) \cdot \vec{u}_i(0)) \rangle \quad (1)$$

where P_l is the l -order Legendre polynomial and \vec{u}_i is a unit vector directed along the C_3 -symmetry carbon-carbon molecular axis of the DFTCE molecule i (see Fig. 1). From $C_{l=1,2}$, we can obtain clarification on the nature of dynamical changes and anisotropy of the molecular motions. Experimentally, $C_1(t)$ can be directly measured in dielectric relaxation and $C_2(t)$ in Raman scattering [31]. $C_{l=1,2}$ can also be related to the informations obtained from NMR relaxation measurements [21].

In order to investigate collective dynamics, the intermediate scattering function as it can be classically obtained from coherent neutron scattering experiments will be mainly considered:

$$S(\vec{Q}, t) = \langle \rho_{\vec{Q}}(t) \rho_{\vec{Q}}(0) \rangle \quad (2)$$

where $\rho_{\vec{Q}}(t)$ is the time-dependent density correlator:

$$\rho_{\vec{Q}}(t) = \sum_{\alpha} b_{\alpha} \exp[i\vec{Q} \cdot \vec{r}_{\alpha}(t)] \quad (3)$$

where the sum is over all the atoms α of the system. b_{α} and \vec{r}_{α} are the coherent scattering length and the position of the α atom respectively. An average over isotropically distributed Q -vectors having the same modulus Q is performed in order to obtain $S(Q, t)$ for a polycrystalline sample. In general, $S(Q, t)$ can be expressed as [32]:

$$S(Q, t) = S_c(Q) + S_d(Q, t) \quad (4)$$

where $S_c(Q) = |\langle \rho_{\vec{Q}} \rangle|^2$ is the coherent elastic scattering and

$$S_d(Q, t) = \langle \delta \rho_{\vec{Q}}(t) \delta \rho_{\vec{Q}}(0) \rangle \quad (5)$$

where $\delta \rho_{\vec{Q}}(t) = \rho_{\vec{Q}}(t) - \langle \rho_{\vec{Q}} \rangle$ is the fluctuation of the time-dependent density operator. For plastic crystals, $S(Q, t)$ is identical to $S_d(Q, t)$ except for Q -vectors corresponding to Bragg peaks for which the long time limit of $S(Q, t)$ reaches the non-zero value $S_c(Q)$. This behaviour is found at all temperatures and it is associated to the crystalline order of the TDOF and not the freezing process of the ODOF. Similarly to the intermediate scattering function, the static correlator can be decomposed into two components $S(Q) = S_c(Q) + S_d(Q)$ where $S_d(Q)$ is the diffuse scattering:

$$S_d(Q) = \langle |\delta \rho_{\vec{Q}}|^2 \rangle = \langle |\rho_{\vec{Q}}|^2 \rangle - |\langle \rho_{\vec{Q}} \rangle|^2 \quad (6)$$

III. RESULTS AND DISCUSSION

A. Static

Owing the high rotational disorder, plastics crystals yield only a few diffraction peaks but exhibit intense and highly structured diffusive scattering which provides useful information to characterize rotational motions and most probable orientations [32]. Fig. 1 shows both numerical and experimental static structure factors obtained in the Q -range $[0.3 - 6.5] \text{ \AA}^{-1}$. The diffraction pattern of the plastic phase presents eight Bragg peaks localized at 1.272, 1.799, 2.203, 2.543, 2.844, 3.114, 3.596 and 3.816 \AA^{-1} which are well indexed as a bcc structure having a cell parameter of 6.985 \AA^{-1} . The cell parameter is found 2% smaller from MD simulation. This result confirms the preliminary X-ray diffraction investigation of this crystal performed by Kishimoto *et Al* [27]. The elastic and the diffuse scattering have been extracted from the MD study and are found in good agreement with the X-ray experiment: maxima of $S_c(Q)$ coincide with the position of the experimental Bragg peaks and maxima of $S_d(Q)$ with the broad bumps of the diffuse scattering at $Q \simeq 1.3, 2.34, 3.36$ and 4.8 \AA^{-1} . It should be mentioned that an additional diffuse scattering bump is observed experimentally close to $Q \simeq 1.6 \text{ \AA}^{-1}$. This feature which is also present in the pattern of the liquid phase (see Fig. 1) mainly derives from the scattering contribution of the glass capillary sample holder. Moreover, a strong similarity of the X-ray pattern is observed between the liquid and plastic phase. Such remarkable feature has been already reported for ethanol [33] or CBr_4 [32]. The first sharp diffraction peak of the liquid particularly corresponds to the first and most intense Bragg peak of the plastic phase. Broad bumps of the diffuse scattering are found almost identical in both phases and merge at the largest Q -vectors since the same intramolecular structure is probed. This result could suggest a strong analogy between the supercooled liquid and the supercooled plastic crystal of the same compound in the framework of the MCT which predict

that dynamics are controlled by non trivial static correlations. This question will be adressed in an other paper [34].

The orientational distribution of the DFTCE molecules can be described with the probability distribution function $f(\vec{u})$ where $\vec{u} = (x, y, z)$ is a unit vector along the carbon-carbon molecular axis of DFTCE (see Fig. 1). Since the site symmetry of the crystal is O_h , $f(\vec{u})$ may be expanded as a series of cubic harmonics K_i [35]:

$$f(\vec{u}) = \frac{1}{4\pi} \left(1 + \sum_{i=4,6,8,\dots} \langle K_i \rangle K_i \right) \quad (7)$$

where $K_4 = (21/16)^{1/2}(5Q - 3)$, $K_6 = (13/128)^{1/2}(462R + 21Q - 17)$ and $K_8 = (561/1024)^{1/2}(65Q^2 - 208R - 94Q + 33)$ with $Q = x^4 + y^4 + z^4$ and $R = x^2y^2z^2$. The $\langle K_i \rangle$ coefficients are the averages of the corresponding K_i . K_4 , K_6 and K_8 have been calculated from MD simulations at different temperatures and are reported in table II. This table clearly shows no strong ordering of the DFTCE molecules along the preferred [111], [110] or [100] directions of the cubic lattice consistent with the high rotational disorder of plastic phases. However, a slight preference for [111] directions is observed. Upon lowering the temperature, we also found an increase of the orientational probability along [111] unlikely to [110] or [100]. These results have been also confirmed from different snapshots of individual molecule trajectories as displayed in Fig 2.

B. Single-molecule reorientational dynamics

Single molecule reorientational dynamics have been investigated from the self angular correlation functions $C_{l=1,2}$ defined in Eq. 1. Figure 2 shows $C_2(t)$ time correlation functions for all investigated temperatures from 130 K to 260 K. $C_1(t)$ time correlation functions, not displayed in the present paper, shows a very similar behaviour to the $C_2(t)$ functions. At high temperatures,

$C_2(t)$ rapidly decays zero and can be described by a simple exponential shape. When lowering the temperature, dynamics slow down and a two-step process is seen as already observed in chloroadamantane plastic crystals [21, 23] and in supercooled liquids [24]. This process is often interpreted in term of $\alpha - \beta$ relaxations which will be carefully analyzed in the next section for collective dynamics in the framework of MCT. Reorientation times τ_1 and τ_2 have been extracted from the time it takes for their respective self angular correlation functions $C_{l=1,2}$ to decay e^{-1} of their initial values. The ratio τ_1/τ_2 is displayed in Fig. 2. For uncorrelated small angular steps motion, it can be shown that $C_l(t)$ functions follow an exponential decay $exp[-t/\tau_l]$ where $1/\tau_l = l(l+1)D_r$ and D_r is the rotational diffusion coefficient. At high temperatures, τ_1/τ_2 is close to the value of 3 in good agreement with this simple diffusion model. Upon lowering the temperature, τ_1/τ_2 clearly deviates from 3 and approaches 1. In [36], we have shown that this behaviour indicates a crossover to large angle tumbling motions. Similar features have been recently shown from MD simulations of supercooled liquid CS_2 [37]. This result is also confirmed from snapshots of single-molecule trajectories in Fig. 2. Thus, low temperature rotational dynamics can be seen as tumblings between preferred orientations along [111] directions of the cubic cell. This result also proves that simple exponential decay for $C_l(t)$ function is not granted at low temperature and that non-exponential relaxations occur.

C. Collective dynamics

The coherent intermediate scattering function $S(Q, t)$ has been calculated from MD at different temperatures and different Q wave-vectors and it is compared with the NSE data in Fig. 3 at the arbitrary wave-vector $Q = 1.54 \text{ \AA}^{-1}$. A good agreement between experimental and numerical $S(Q, t)$ is found. However, some discrepancies are particularly observed at high temperatures at the longest Fourier times for which the NSE $S(Q, t)$ does not decay completely to zero. Since no

elastic contribution is expected outside the Bragg Peaks, this feature is most likely due to uncertainties in the background subtraction. At low temperatures, at $T = 130$ and 140 K, difference between experiment and simulation are also seen. Those are also the data which show the largest error bars. One explanation could be the use of a different sample (see experimental details) providing a less intense scattering signal.

Upon cooling, $S(Q, t)$ displays a decay classically observed in MD simulations [12] and in NSE experiments of glass-forming molecular liquids such as glycerol [38] or CKN [39]. For DFTCE glassy crystal, the long time relaxation corresponding to the overall rotations of molecules is separated from short time regime by a plateau-like region. This latter can be associated to the orientational trapping of molecules, the analogue of the cage effect in liquids [40], as already demonstrated in [36] for others plastic crystals. In the long time relaxation regime, we defined the characteristic time $\tau_{1/e}$ of the rotational dynamics as the time it takes for $S(Q, t)$ to decay from 1 to $1/e$ at the wave-vector $Q = 1.54 \text{ \AA}^{-1}$. This arbitrary definition is chosen in order to fully compare both NSE and MD data. Owing the limited Q and time domain investigated in the present NSE experiment, other definitions such as fits with stretched exponential of Kohlrausch or time measured to decay from 1 to 0.1 can not be employed. An alternative definition will be particularly used in the following section concerning the MCT analysis of the MD data.

$\tau_{1/e}$ obtained experimentally and numerically are displayed in Fig. 4. We found that both NSE and MD characteristic times $\tau_{1/e}$ are consistent with previous NMR [29] and dielectric investigations[28] and allows us to extend DFTCE data at high temperatures over 3-4 decades. It clearly confirms the non-Arrhenius behavior of the rotational dynamics. For comparison, we also plotted in Fig. 5, the Vogel-Fulcher-Tammann (VFT) law $\tau_{VFT} = \tau_{\infty} \exp[1/K_{VFT} \cdot (T/T_{VFT} - 1)]$ where T_{VFT} is the temperature of apparent divergence of τ_{VFT} and K_{VFT} measures the kinetic fragility. Parameters $K_{VFT} = 0.13$ and $T_{VFT} = 70$ K were determined from dielectric exper-

iments of plastic DFTCE [28] in the temperature range [95-120] K. From MD simulation, we obtained $K_{VFT} \simeq 0.20$ and $T_{VFT} \simeq 86.9$ K for $\tau_{1/e}$ in fair agreement with the dielectric experiment. A perfect agreement can not be expected owing the Q -dependence of the neutron scattering technique and the different temperature domain investigated.

In [23, 36], we suggested that some common microscopic mechanisms, relatively well described by MCT, are involved in both orientationally disordered crystals and molecular liquids. Therefore, in the following, we analyse our data in the MCT framework. In Fig. 6, $S(Q, t)$ is plotted against the rescaled time $\tau_{1/e}$ previously determined. We find that one of the main predictions of MCT *i.e* the time-temperature superposition principle (TTSP) holds relatively well both for NSE and MD data. We show that the curves overlap for the large time part and collapse gradually onto a master curve upon cooling. This feature is made particularly clear since we have developed a realistic MD model of DFTCE which allows us to access data in the plateau region of $S(Q, t)$ which was not possible in the present NSE experiment. At $T = 130$ K, $S(Q, t/\tau_{1/e})$ obtained from MD deviates from the master curve. This indicates that MCT ceases to be valid at that temperature. This result is confirmed from snapshots and trajectories of target molecules, as already shown for other plastic crystals in [16, 36], which reveal that at the lowest temperatures rotational motions correspond to activated tumblings of the overall molecules between preferred molecular orientations *i.e* the so-called hopping processes not taken into account in the ideal version of MCT (see section III A). Moreover, this deviation also allows us to roughly estimate the critical temperature T_c .

Above T_c , MCT predicts that the late β regime or the early α relaxation is described by the following power law (going beyond first order):

$$\phi(Q, t) = f_Q^c - h_Q^{(1)} \cdot (t/\tau)^b + h_Q^{(2)} \cdot (t/\tau)^{2b} \quad (8)$$

where f_Q^c is the so-called nonergodicity parameter associated to the plateau height and $\tau = t_0(T -$

$T_c)^{-\gamma}$ with $\gamma = 1/2a + 1/2b$. The parameters $t_{0,\gamma}$ and b are temperature and q independent and related via $\gamma = 1/2a + 1/2b$ and $\Gamma^2(1 - a)/\Gamma(1 - 2a) = \Gamma^2(1 + b)/\Gamma(1 + 2b)$ where $\Gamma(x)$ is the gamma function. The first two terms of Eq. 8 correspond to the classical von Schweidler law and the last term is a second order correction. First, we fixed the exponent b by performing individual fits of the different correlators $S(Q, t)$ in the late β regime using Eq. 8 at $T = 140$ K expected to be the lowest temperature where MCT predictions are valid (see Fig. 5). We used the following free parameters: $b, f_Q^c, \tilde{h}^{(1)} = h^{(1)}(Q) \cdot \tau^{-b}$ and $\tilde{h}^{(2)} = h^{(2)}(Q) \cdot \tau^{-2b}$. Best results are obtained for $b = 0.59$ which corresponds to $a = 0.31$ and $\gamma = 2.45$. Then, using this value of γ , scaling properties in the α relaxation regime have been checked using two functions $R_1(T)$ and $R_2(T)$ defined as:

$$R_1(T) = \frac{\tau_Q^{-1/\gamma}(T) - \tau_Q^{-1/\gamma}(T_1)}{\tau_Q^{-1/\gamma}(T_2) - \tau_Q^{-1/\gamma}(T_1)}(T_2 - T_1) + T_1 \quad (9)$$

$$R_2(T) = \frac{\tau_Q^{-1/\gamma}(T)}{\tau_Q^{-1/\gamma}(T_2) - \tau_Q^{-1/\gamma}(T_1)}(T_2 - T_1) \quad (10)$$

where T_1 and T_2 are two arbitrary low temperatures and $\tau_Q(T)$ is a characteristic time of the α relaxation defined as the time it takes for $S(Q, t)/S(Q, t = 2 \text{ ps})$ to decay from 1 to $1/e$. This alternative definition eliminates the short-time dynamics and ensures that the β relaxation does not perturb the α -relaxation time *i.e.* $\tau_Q(T)$ is not influenced by other parameters $f_Q, h^{(1)}(Q)$ or b . Therefore, it avoids a tedious fitting procedure with stretched exponential of Kohlrausch. It is also assumed that any characteristic times belonging to the α regime show asymptotically the same temperature dependence $\tau_Q \sim \tau$ defined in Eq. 8. For all Q vectors, it can be shown that $R_1(T) = T$ and $R_2 = T - T_c$ in the temperature range where MCT predictions are valid. In Fig. 6, R_1 and R_2 scaling functions are displayed as function of temperature at different Q wave vectors. They clearly indicate a temperature range [140-180] K where all data obey an universal master curve. This result is particularly significant owing the wide Q -range investigated and confirms

the choice for the exponent b . Both R_1 and R_2 allow us to estimate two remarkable temperatures: i) $T_A \simeq 180$ K corresponding to the crossover from simple liquids dynamics to slow dynamics. As observed in previous MD of molecular glass-forming liquids [24], polymer melts [41] or plastic crystals [23], this temperature seems very dependent on the chosen correlator $S(Q, t)$ *i.e* on the space range probed at the wave-vector Q . ii) the critical temperature predicted by MCT $T_c \simeq 128$ K. The superposition of the different correlators seems better for R_1 than R_2 . Thus, contrary to MCT predictions, this reveals a weak Q -dependence of T_c of about 3 K. In order to check the limit of this approach, the same work was also performed on the NSE data and results are displayed as inset in Fig 6. It should be mentioned that τ_Q is not accessible in our present experimental data and we had to use $\tau_{1/e}$ which is intrinsically worse. $\tau_{1/e}$ is influenced by the β -regime. Moreover, b obtained from MD was employed. Despite these two drawbacks, reasonable results are obtained for both R_1 and R_2 for the narrow Q -range investigated in fair agreement with the MD data and clearly motivate measurement at shorter times using time-of-flight experiment to describe the plateau regime.

A fundamental property of MCT or MMCT stresses that dynamics are driven by the static density correlator $S(Q)$. This has been confirmed in several numerical and experimental studies for simple [42] or molecular [12, 43] glass-forming liquids. Since a good agreement between experiment and simulation was found for the elastic and the diffuse structure factor (see Fig. 1), we checked the Q -dependence of the α -relaxation time τ_Q , the non-ergodicity parameter f_Q and the total prefactors $\tilde{h}^{(1)}(Q)$ and $\tilde{h}^{(2)}(Q)$ at $T = 160$ K. Results are shown in Fig. 7. Clearly, we found that τ_Q , f_Q oscillate in phase with $S_d(Q)$ and $S_c(Q)$ while the amplitudes $\tilde{h}^{(1)}(Q)$ and $\tilde{h}^{(2)}(Q)$ oscillate in phase with $S_d(Q)$ and out of phase with $S_c(Q)$. It should be noted that the Q -modulation of the non-ergodicity parameter and the total prefactor strongly resembles to results obtained by Franosch *et Al.* for a hard-sphere colloidal suspension model [44].

IV. CONCLUSION

In this paper, we have investigated static and dynamical properties of difluorotetrachloroethane glassy crystal using complementary X-ray and NSE experiments and MD simulations performed for a realistic molecular model. This study clearly confirms that supercooled molecular liquids and supercooled orientationally disordered crystal share many properties in the ps-ns regime where some precursor features (non-exponentiality or non-Arrhenius behavior) of the glass transition emerge. We particularly found that some MCT equations developed for atomic liquids provide a good description of rotational dynamics: some MCT predictions such as the superposition principle or the power law $(T - T_c)^{-\gamma}$ dependence ($T_c \simeq 128$ K) of the α -relaxation time characterizing collective dynamics hold well. We also demonstrated that the α -relaxation time τ_Q , the non-ergodicity parameter f_Q and the amplitudes $h_1(Q)$ were modulated by the static correlation consistent with the MCT predictions. In addition, the other remarkable temperature T_A was detected at about 180 K for both self and collective dynamics. Therefore, in order to fully validate the MD results, it will be of great interest: i) to complete the present NSE study over a wider Q -range and for longer Fourier times in order to reach the estimated T_c and ii) to make measurement at shorter times using time-of-flight experiment to describe the plateau regime.

Acknowledgments

The authors wish to acknowledge the use of the facilities of the IDRIS (Orsay, France) and the CRI (Villeneuve d'Ascq, France) where calculations were carried out. This work was supported

by the INTERREG III program (Nord Pas de Calais/Kent).

- [1] P. G. Debenedetti and F. H. Stillinger, *Nature* **410**, 259 (2001).
- [2] S. Sastry, *Nature* **409**, 164 (2001).
- [3] J. Kim, W. Lee, and T. Keyes, *Phys. Rev. E* **67**, 021506 (2003).
- [4] W. Götze, in *Liquids Freezing and the Glass Transition*, J. P. Hansen, D. Levesque and J. Zinn-Justin (North-Holland, 1990).
- [5] R. Schilling, in *Collective Dynamics of Nonlinear and Disordered Systems*, G. Radons, W. Just, and P. Haeussler (Springer, 2003).
- [6] G. Heuberger and H. Sillescu, *J. Phys. Chem.* **100**, 15255 (1996).
- [7] F. R. Blackburn, C.-Y. Wang, and M. Ediger, *J. Phys. Chem.* **100**, 18249 (1996).
- [8] S.-H. Chong, W. Götze, and A. Singh, *Phys. Rev. E* **63**, 011206 (2001).
- [9] R. Schilling and T. Scheidsteger, *Phys. Rev. E* **56**, 2932 (1997).
- [10] L. Fabbian, A. Latz, R. Schilling, F. Sciortino, P. Tartaglia, and C. Theis, *Phys. Rev. E* **60**, 5768 (1999).
- [11] S.-H. Chong and F. Sciortino, *Europhys. Lett.* **64**, 197 (2003).
- [12] S.-H. Chong and F. Sciortino, *Phys. Rev. E* **69**, 051202/1 (2004).
- [13] U. T. Höchli, K. Knorr, and A. Loidl, *Adv. Phys.* **39**, 405 (1990).
- [14] K. H. Michel, *Z. Phys. B, Cond. Mat.* **68**, 259 (1987).
- [15] H. Suga and S. Seki, *J. of Non-Cryst. Solids* **16**, 171 (1974).
- [16] F. Affouard, J.-F. Willart, and M. Descamps, *J. of Non-Cryst. Solids* **307-310**, 9 (2002).
- [17] A. Criado, M. Jimenez-Ruiz, C. Cabrillo, F. J. Bermejo, R. Fernandez-Perea, H. E. Fischer, and F. R. Trouw, *Phys. Rev. B* **61**, 12082 (2000).
- [18] S. Benkhof, A. Kudlik, T. Blochowicz, and E. Rössler, *J. Phys.: Condens. Matter* **10**, 8155 (1998).

- [19] M. Winterlich, G. Diezemann, H. Zimmermann, and R. Böhmer, *Phys. Rev. Lett.* **91**, 235504/1 (2003).
- [20] R. Brand, P. Lunkenheimer, and A. Loidl, *Phys. Rev. B* **56**, 5713 (1997).
- [21] F. Affouard, E. Cochín, R. Decressain, and M. Descamps, *Europhys. Lett.* **53**, 611 (2001).
- [22] F. Affouard, A. Hédoux, Y. Guinet, T. Denicourt, and M. Descamps, *J. Phys.: Cond. Matter* **13**, 7237 (2001).
- [23] F. Affouard and M. Descamps, *Phys. Rev. Lett.* **87**, 035501/1 (2001).
- [24] S. Kämmerer, W. Kob, and R. Schilling, *Phys. Rev. E* **56**, 5450 (1997).
- [25] C. D. Michele and D. Leporini, *Phys. Rev. E* **63**, 036702/1 (2001).
- [26] S.-H. Chong and W. Götze, *Phys. Rev. E* **65**, 041503/1 (2002).
- [27] K. Kishimoto, H. Suga, and S. Seki, *Bull. Chem. Soc. Japan* **51**, 1691 (1978).
- [28] J. K. Krüger, J. Schreiber, R. Jimenez, and K.-P. Bohn, *J. Phys.: Condens. Matter* **6**, 6947 (1994).
- [29] H. Stokes, T. Case, D. Ailion, and C. Wang, *J. Chem. Phys.* **70**, 3563 (1979).
- [30] M. Evain, P. Deniard, A. Jouanneaux, and R. Brec, *J. Appl. Cryst.* **26**, 563 (1993).
- [31] J. N. Sherwood, *The Plastically Crystalline State* (J. Wiley & Sons, 1979).
- [32] G. Dolling, B. M. Powell, and V. F. Sears, *Mol. Phys.* **37**, 1859 (1979).
- [33] R. Fayos, F. J. Bermejo, J. Davidowski, H. E. Fischer, and M. A. Gonzalez, *Phys. Rev. Lett.* **77**, 3823 (1996).
- [34] F. Affouard and M. Descamps, In preparation (2005).
- [35] R. Chelli, G. Cardini, and S. Califano, *J. Chem. Phys.* **107**, 8041 (1997).
- [36] F. Affouard and M. Descamps, *Phys. Rev. B* **59**, 9011 (1999).
- [37] J. Kim and T. Keyes, *J. Chem. Phys.* **121**, 4237 (2004).
- [38] J. Wutke, W. Petry, and S. Pouget, *J. Chem. Phys.* **105**, 5177 (1996).
- [39] F. Mezei, W. Knaak, and B. Farago, *Phys. Rev. Lett.* **58**, 571 (1987).

- [40] P. Bordat, F. Affouard, M. Descamps, and F. Müller-Plathe, *J. Phys.: Cond. Matter* **15**, 5397 (2003).
- [41] M. Aichele and J. Baschnagel, *Eur. Phys. J. E.* **5**, 245 (2001).
- [42] W. Kob and H. C. Andersen, *Phys. Rev. E* **52**, 4134 (1995).
- [43] S. Mossa, G. Ruocco, and M. Sampoli, *Phys. Rev. E* **64**, 021511 (2001).
- [44] T. Franosch, M. Fuchs, W. Götze, M. R. Mayr, and A. P. Singh, *Phys. Rev. E* **55**, 7153 (1997).

Tables captions

TABLE I: Simulation coefficients taken from literature for Buckingham potential $\phi(r) = A \exp(-\rho \cdot r) - C/r^6$.

TABLE II: Orientational order parameters $\langle K_4 \rangle$, $\langle K_6 \rangle$ and $\langle K_8 \rangle$ at different temperatures. Values for pure [111], [110] and [100] ordering are also indicated.

TABLE 1

Site-Site	A (kJmol ⁻¹)	ρ (Å ⁻¹)	C (kJmol ⁻¹ Å ⁶)
C - C	226307	0.288	2420
C - F	196747	0.260	1168
C - Cl	390940	0.284	3864
F - F	171038	0.237	565
F - Cl	320883	0.258	1808
Cl - Cl	586389	0.284	5798

TABLE 2

Temperature	$\langle K_4 \rangle$	$\langle K_6 \rangle$	$\langle K_8 \rangle$
140	-0.647	0.465	0.211
160	-0.638	0.409	0.191
180	-0.623	0.368	0.173
200	-0.596	0.319	0.151
220	-0.577	0.291	0.134
240	-0.549	0.257	0.120
260	-0.515	0.223	0.105
[111]	-1.528	2.266	0.877
[110]	-0.573	-2.071	1.665
[100]	2.291	1.275	2.961

Figures captions

FIG. 1: Experimental X-ray powder diffraction pattern in the liquid phase at $T = 305$ K (top) and the plastic phase at $T = 140$ K (bottom) as function of the wave-vector Q . The calculated coherent elastic scattering $S_c(Q)$ (dotted line) and the calculated diffuse scattering $S_d(Q)$ (dashed line) in the plastic phase are also indicated for comparison. The DFTCE molecule is displayed in inset.

FIG. 2: Trajectories (top) of the unit vector $\vec{u}(t) = (x(t), y(t), z(t))$ of one target molecule over a 1 ns run at 140 K (left) and 240 K (right). Horizontal lines indicates preferred orientation of \vec{u} along cubic [111] directions. Ratio (bottom) of reorientational correlation times τ_1 and τ_2 obtained from MD simulation as function of temperature from 130 to 260 K. The reorientational correlation function $C_2(t)$ as function of time at different temperatures from 130 to 260 K is given in inset.

FIG. 3: Coherent intermediate scattering function $S(Q, t)$ at $Q = 1.54 \text{ \AA}^{-1}$ obtained from Neutron Spin Echo experiments (full circle) and MD computer simulations (solid line) at $T = 130, 140, 150, 160, 180$ and 200 K.

FIG. 4: Characteristic time $\tau_{1/e}$ obtained from NSE experiment (full circle) and MD simulation (open circle) at $Q = 1.54 \text{ \AA}^{-1}$ as function of the temperature. Data extracted from NMR (square) [29] and dielectric experiment using a VFT fit (gray line) [28] are also indicated.

FIG. 5: $S(Q, t)$ obtained from NSE experiment at $Q = 1.54 \text{ \AA}^{-1}$ plotted against the scaled time $t/\tau_{1/e}$ at different temperatures from $T = 140$ to 190 K. $S(Q, t)$ calculated from MD simulation at same Q wave-vectors is displayed at different temperatures from 130 to 220 K.

FIG. 6: Scaling functions R_1 and R_2 at different wave-vectors Q ranging from 0.7 to 3.9 \AA^{-1} as function of the temperature. R_1 and R_2 are defined in Eq. 9 and 10 respectively using exponent $\gamma = 2.45$ extracted from the MCT analysis in the β regime and $T_1 = 140$ K and $T_2 = 170$ K. $R_1(T) = T$ and $R_2(T) = T - T_c$ are expected from MCT predictions. R_1 and R_2 extracted from NSE experiment using characteristic times $\tau_{1/e}$, $T_1 = 150$ K and $T_2 = 190$ K are given in inset.

FIG. 7: Q -dependence of different parameters at the temperature $T = 160$ K. a) The α -relaxation times τ_Q extracted from the $S_d(Q, t)$ correlators. b) and c) The non-ergodicity parameter f_Q and the total prefactor $\tilde{h}^{(1)}(Q)$ obtained from a fitting procedure of $S(Q, t)$ using a von Schweidler law as derived from MCT including second order corrections (see Eq. 8). $\tilde{h}^{(2)}(Q)$ is not shown but exhibits the same Q -dependence as $\tilde{h}^{(1)}(Q)$. d) The diffuse scattering $S_d(Q)$. First Bragg peaks positions clearly identified from MD are also indicated with vertical lines.

FIGURE 1

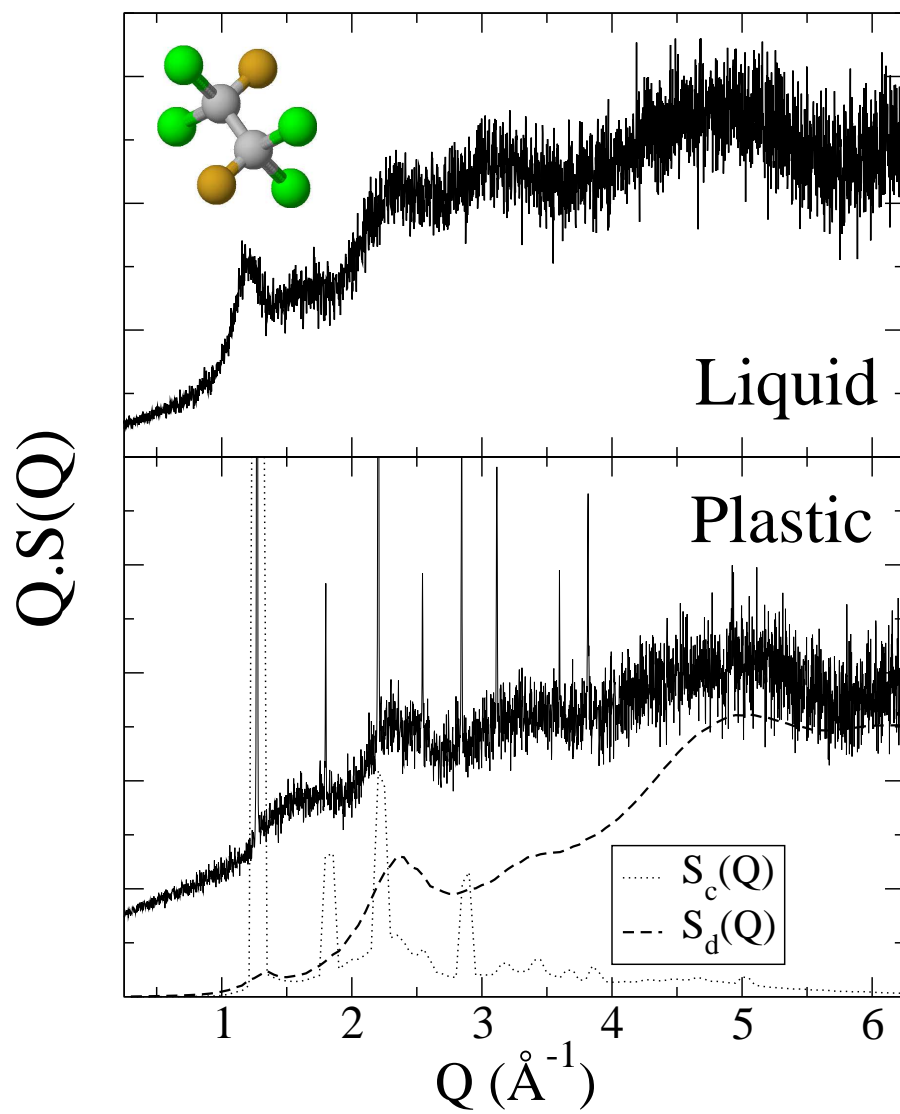


FIGURE 2

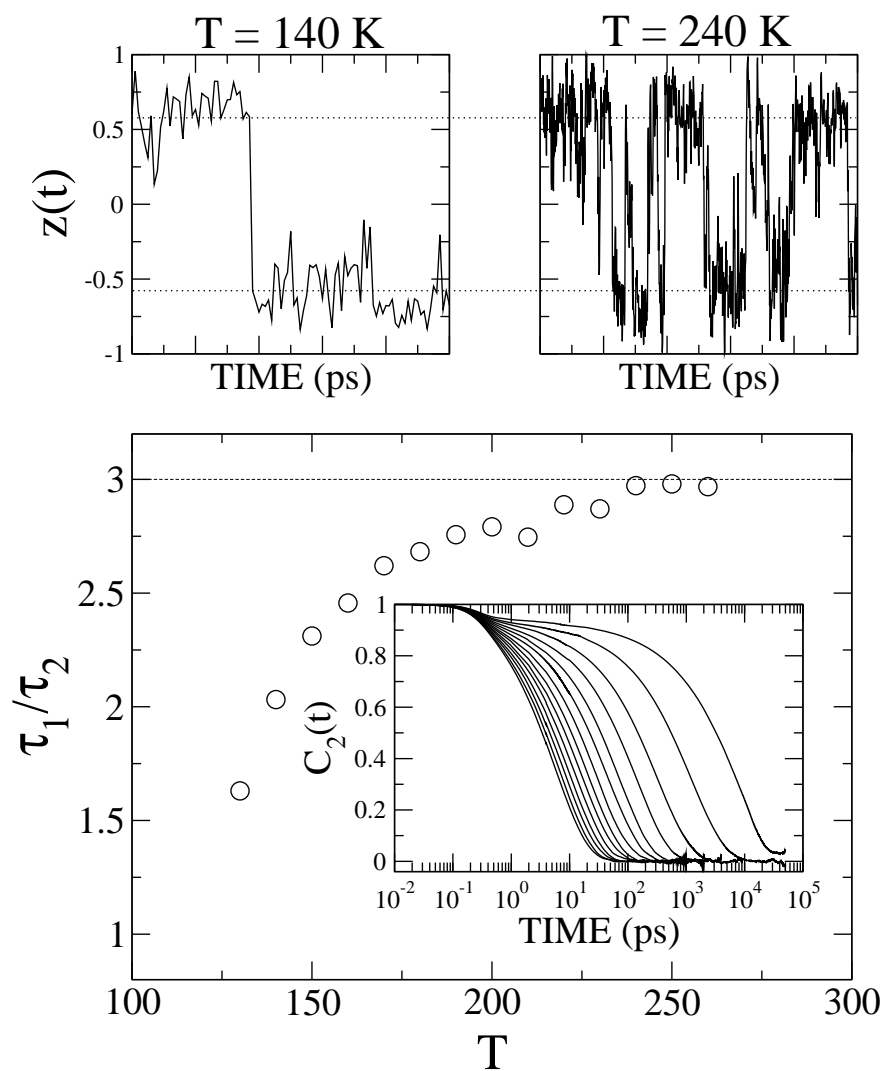


FIGURE 3

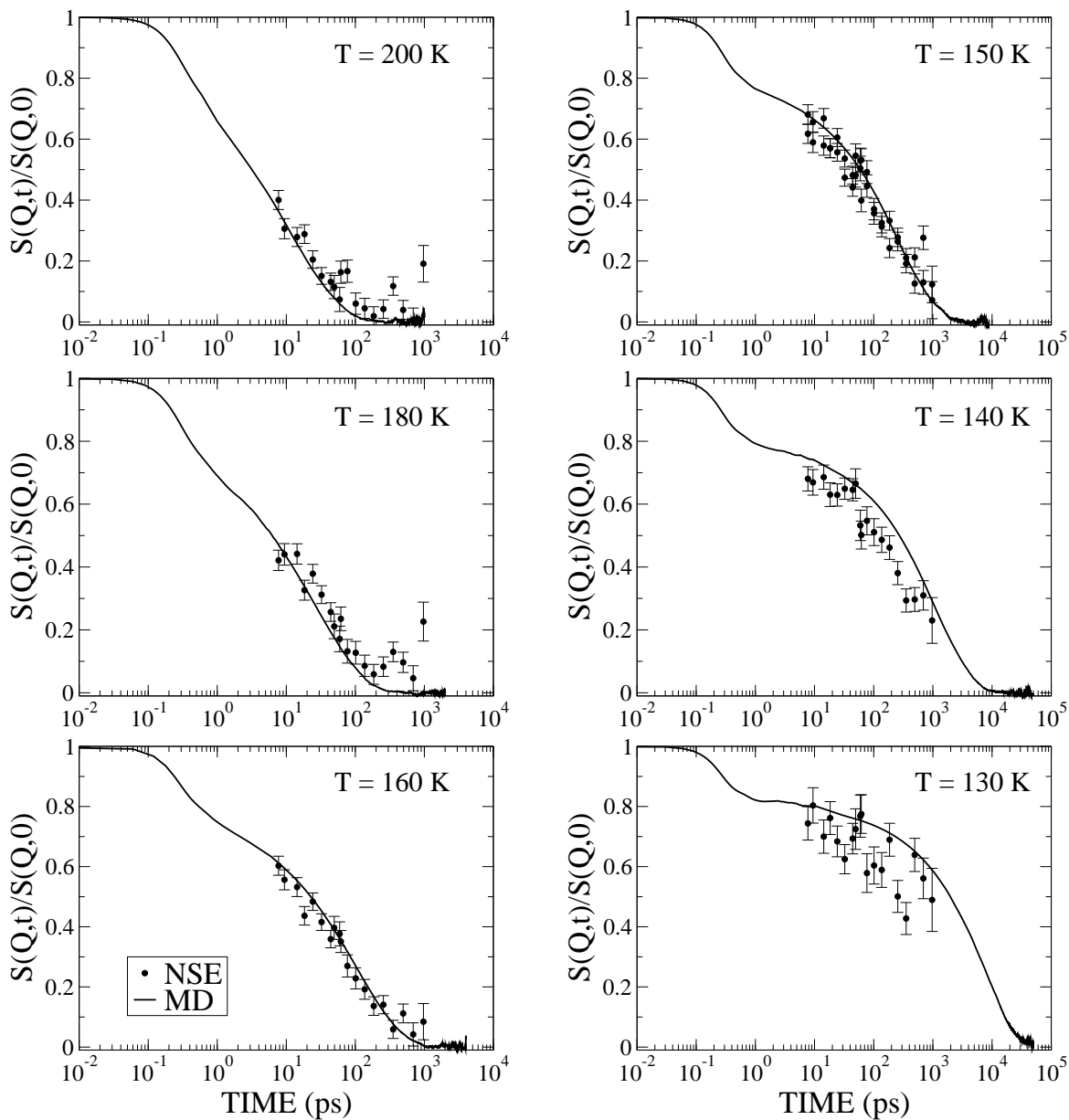


FIGURE 4

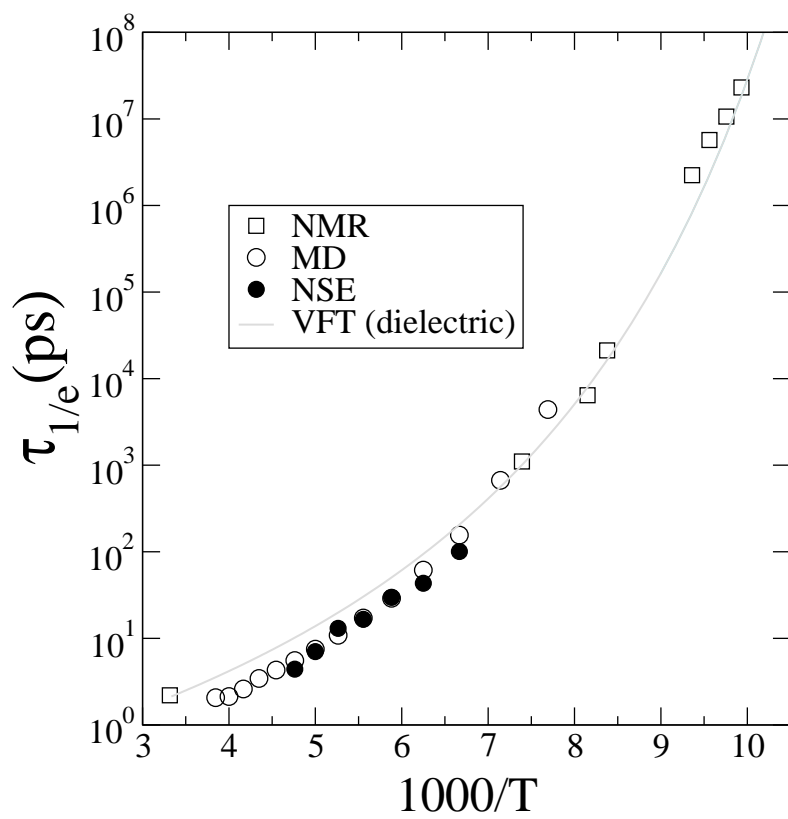


FIGURE 5

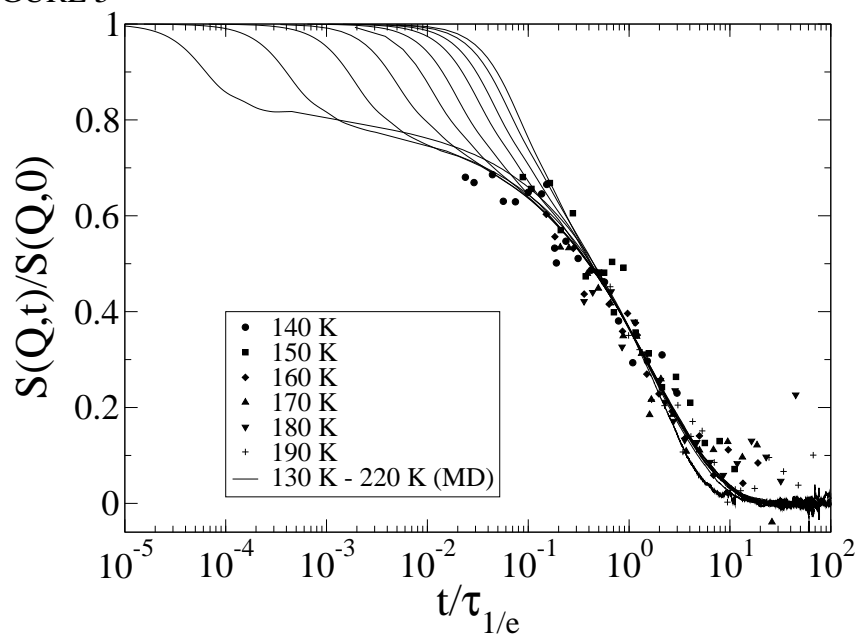


FIGURE 6

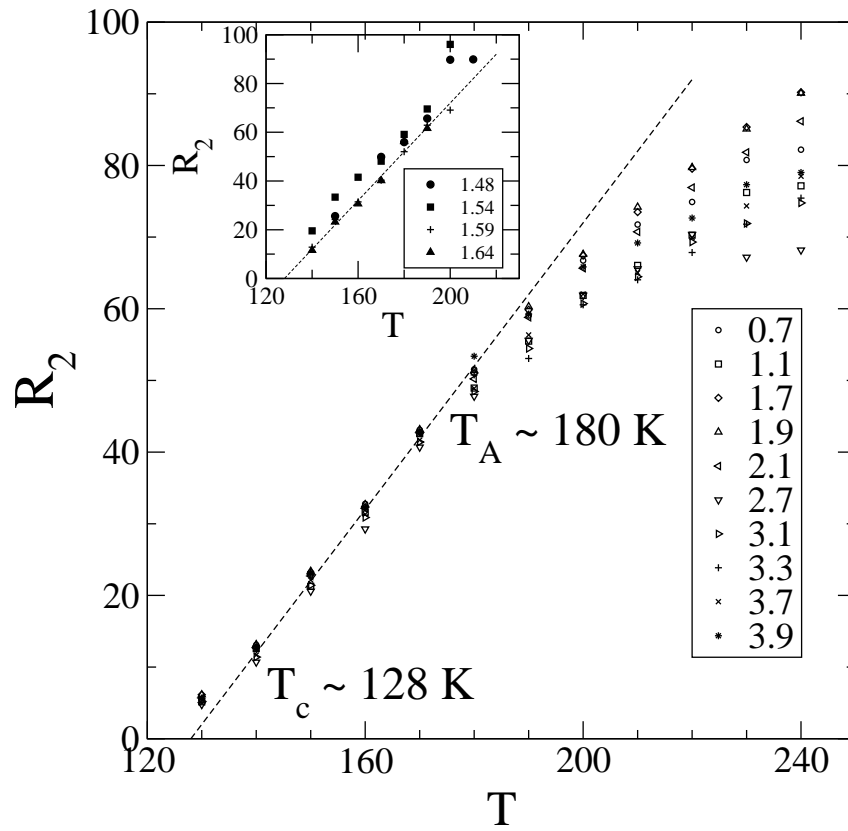
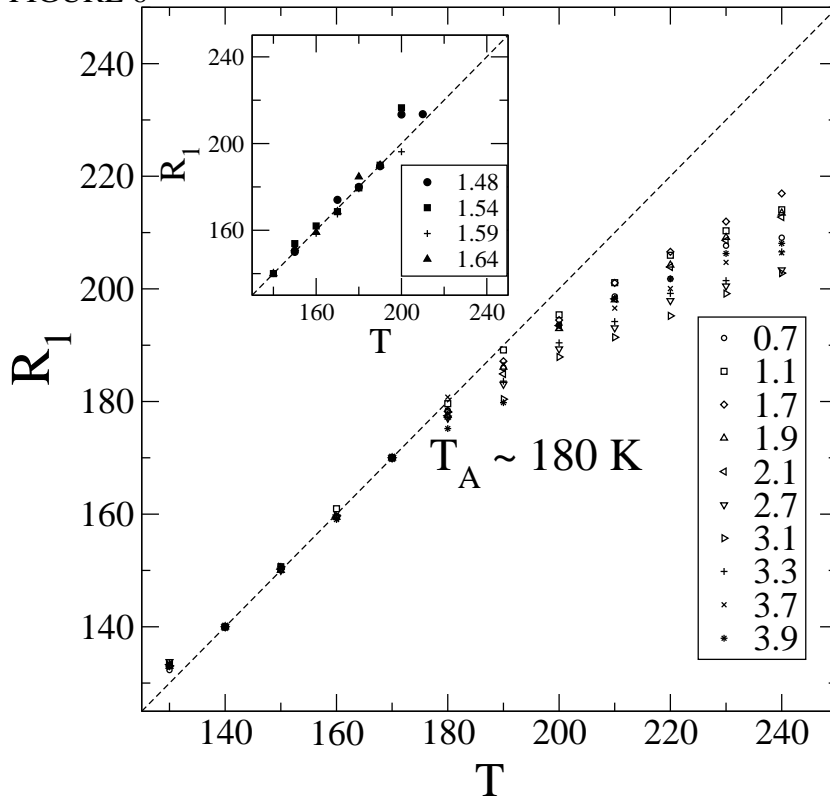


FIGURE 7

